

固體粒子的反應에 관한 模型的 比較

朴 晉 用

서울대학교 공과대학 화학공학과

Comparison of Model for the Reaction of Solid Particles

Jin Y. Park

*Department of Chemical Engineering, College of Engineering
Seoul National University, Seoul 130-02, Korea*

概 要

固體粒子가 氣體와 反應할 때 反應이 reactant 와 product 의 境界面에 局限되지 않아서, 간단한 shrinking core 模型을 適用할 수 없는 경우가 많으며 이때 反應에 따르는 여러 現象을 說明하기 위하여 많은 氣固反應模型이 提案되어 있다. 本報文中에서는 이들 諸 模型을 크게 둘로 分類하고 이중 가장 基本的인 構型, 즉 Szekely 등에 의하여 提案되고 多孔性粒子的 反應에 適合한 grainy porous pellet 模型과 Park 과 Levenspiel 에 의하여 提案되고 非多孔性粒子的 反應에 適合한 Crackling core 模型을 比較하였다. 反應現象을 보는 見解, 反應時間에 따른 轉化率曲線의 形態, 粒子크기의 影響등에 관한 두 模型의 相異點을 檢討하였으며 또한 模型係數의 決定 및 模型의 選擇에 관하여도 言反하였다.

Abstract

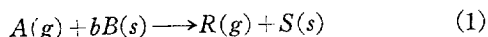
Numerous models have been proposed to account for gas-solid reactions where conversion does not occur at a sharp moving front and where the simple shrinking core model is not applicable. Here we compare the simplest representations of the two broad classes of such models: the grainy porous pellet model of Szekely and coworkers for the reaction of porous particles, and the crackling core model of Park and Levenspiel for the reaction of dense particles. The phenomenological view, the conversion-time behavior and the size dependency are markedly different for these two models. Experimental methods for evaluating the parameters of these models and for choosing the right one for the system at hand are discussed.

Introduction

When a solid particle reacts with its surrounding gas it is sometimes observed that reaction occurs from the outside in, and that a sharp front separates the shrinking core of unattacked virgin solid and the growing shell of completely converted product solid. The two limiting rate controlling mechanisms are either the attack and destruction of the virgin core (reaction control) or the diffusion of gaseous reactant through the product layer (ash diffusion control).

This model, called the *shrinking core model*, in one or other of its forms, has been introduced and forgotten a number of times in the early part of this century. Eventually, following the publications of Yagi and Kunii¹⁾, McKewan²⁾, Levenspiel³⁾, Spitzer, *et al.*⁴⁾ this model became firmly established in the mainstream of chemical and metallurgical engineering.

Basically this model views that the porosity of the reactant solid is rather small and hence reactant solid is practically impervious to reactant gas, and that the fragments of solid formed by fissures and cracks on the surface of virgin core are converted very rapidly so that the moving reaction front leaves behind it completely converted solid. For stoichiometry



We obtain³⁾ from this model the following simple conversion-time expressions for spherical reacting particles: For reaction control

$$\frac{t}{\tau} = 1 - (1-X)^{1/3}; \quad \tau = \frac{\rho_B R^2}{bk_s C_A} \quad (2)$$

For ash diffusion control

$$\frac{t}{\tau} = 1 - 3(1-X)^{2/3} + 2(1-X); \quad \tau = \frac{\rho_B R^2}{6bDC_A} \quad (3)$$

where τ is the time required for complete

conversion.

Fig. 1 shows how the conversion of solid changes with time for this model, and a plot of the l. h. s. versus the r. h. s. of either of the above expressions provides a simple test for the predictions of the model.

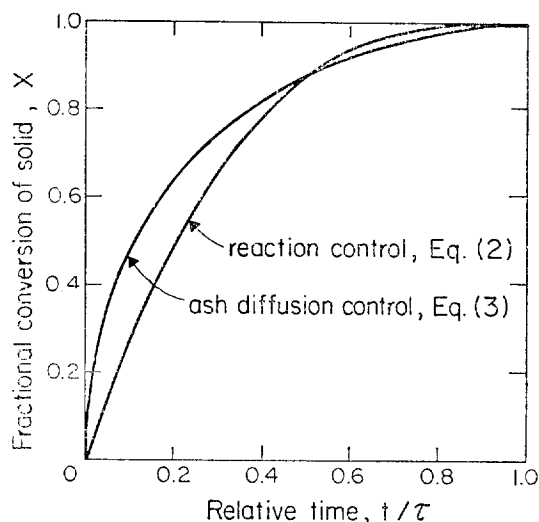


Fig. 1. Conversion of solid versus time of reaction for the shrinking core model.

This model is very attractive and is widely used because its equations are simple and because it is easy to test its predictions against experiment.

Unfortunately, however, observations of real reacting particles often show that the reaction front between the virgin solid and the product shell is not sharp and distinct but is rather broad, even spreading across the whole pellet. In the extreme case reaction occurs uniformly throughout the pellet as the homogeneous reaction model³⁾ predicts.

Numerous models have been proposed to account for these observations. Most of these fall into two general classes: the porous pellet model (Ishida and Wen⁵⁾, Tien and Turkdogan⁶⁾, Sohn and Szekely^{7,8)} and Pigford and Sliger⁹⁾ and the dense pellet model (Park and

Levenspiel¹⁰).

The *porous pellet model* views that the solid is initially porous and thus the gas penetrates into and reacts with the reactant solid producing partly converted solid ahead of the growing ash layer. On the other hand, the *dense pellet model* views that the solid is initially nonporous; cracks first form at the pellet surface and penetrate into the interior; and as a result the virgin core shrinks leaving behind a grainy structure which then reacts away.

Fig. 2 illustrates these two types of models and compares their wide reaction zones with the sharp interface of the shrinking core model and with the uniform reaction zone of the homogeneous reaction model.

These two distinct mechanisms have in fact long been recognized, and indeed there exists much experimental evidence in support of each mechanism. The reaction of pelletized porous particles¹¹ is a typical example for the porous pellet model while a very slow reaction of entrapped "islets" of wustite behind the shrinking virgin core of natural dense iron ores^{12,13,14} supports the dense pellet model.

Although much more complex representations are available, in this paper we will only compare the simplest of these two classes of mechanisms: on the one hand, the *grainy porous pellet model* of Sohn and Szekely^{7,8} for the

reaction of porous solid; on the other hand, the *crackling core model* of Park and Levenspiel¹⁰ for the reaction of dense solids. These are both two-parameter models.

We will characterize explicitly their different predictions. This will allow a future worker to make simple tests to tell which of these models best fits system.

It is felt that these models will be useful as the first practical extensions of the simple shrinking core model.

Mechanism of attack and conversion expressions

To visualize the mechanism of attack, let a spherical pellet of solid B of radius R be immersed in gaseous A of concentration C_A , let external heat and mass transfer resistances be negligible, and let the pellet be isothermal throughout the reaction process.

Grainy Porous Pellet Model

Sohn and Szekely^{7,8} visualize the pellet as porous and consisting of grains of uniform size and shape. The mechanism of attack is viewed as follows:

1. Gaseous A first diffuses through interstices between grains into the pellet of effective diffusivity D attacking each of the grains of radius r_g , $r_g \ll R$, according to the shrinking core model.

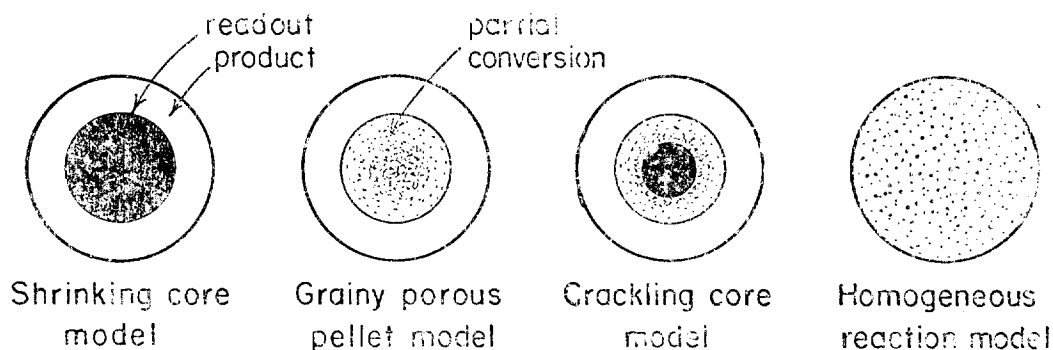


Fig. 2 Comparison of the reaction zones predicted by various models.

- At time τ_g the ash layer first forms on the external surface of the pellet. The ash layer boundary moves into the pellet giving complete conversion of the pellet at time τ .
- The solid structure is macroscopically uniform and is *not* affected by the reaction.
- The rate of attack of the grains is first order with respect to gaseous reactant.

Fig. 3 then illustrates the different stages through which a pellet passes according to this model.

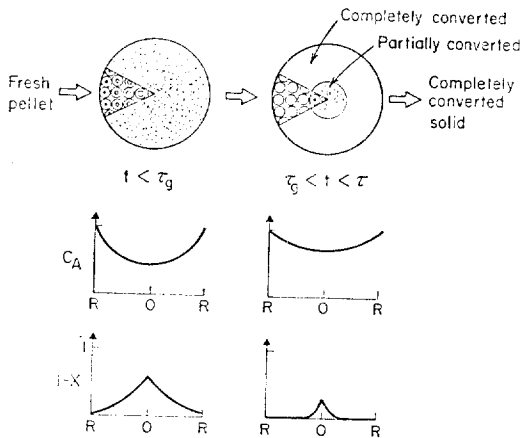


Fig. 3 Progressive stages in conversion of a pellet for the grainy porous pellet model.

The time scales τ and τ_g are two independent parameters for this model; however, in order to elucidate the mechanistic view—diffusion and reaction within the pellet—Sohn and Szekeley introduced a Thiele modulus like parameter σ defined as follows: for reaction control in grain,

$$\sigma \propto R \sqrt{\frac{k_s}{D}} \quad (4)$$

for ash diffusion control in grain,

$$\sigma \propto R \sqrt{\frac{D'}{D}} \quad (5)$$

in which D' is the effective diffusivity of reactant gas in the ash layer of the grain.

Unfortunately, the analysis for this model is not amenable to analytic solution and requires a computer generated numerical solution. With

some reservation, however, Sohn and Szekeley^{7,8)} recommended a method of obtaining approximate working expressions. Thus if τ_d is the time required for complete conversion if the conversion of the conversion of grains were infinitely fast, we have

$$\tau \cong \tau_g + \tau_d = \tau_g + \sigma^2 \tau_g \quad (6)$$

The ratio of times ω may be defined for this two-parameter model as a working parameter along with τ_g :

$$\omega = \frac{\tau_d}{\tau} = \frac{\sigma^2}{1 + \sigma^2} \quad (7)$$

The approximate conversion-time expressions then are given for spherical pellet-spherical grains as follows:

For reaction control in grain:

$$\frac{t}{\tau} \cong (1-\omega) [1 - (1-X)^{1/3}] + \omega [1 - 3(1-X)^{2/3} + 2(1-X)] \quad (8)$$

For ash diffusion control in grain:

$$\frac{t}{\tau} \cong 1 - 3(1-X)^{1/3} + 2(1-X) \quad (9)$$

Whether these approximations are satisfactory for all practical conditions is still uncertain and not yet clearly justified. One might notice here that Eq. (9) is identical to Eq. (3) regardless of ω , which is questionable. There is a current need for a still simple but better method of approximation.

Crackling Core Model

Park and Levenspiel¹⁰⁾ visualize the pellet as initially dense and practically impervious to reactant gas but turns grainy or porous under the action of gas. The mechanism of attack is viewed as follows:

- Gaseous A first attacks the outside of the pellet causing cracks and fissures to form. The attacking front moves steadily into the pellet, and the unattacked core shrinks to zero in time τ_c .
- The solid left after the front passes consists of a porous structure of grains which does

not restrict the passage of gas. Hence reactant gas has a concentration C_A throughout the cracks and fissures.

- Each of the grains then reacts away with gas according to the shrinking core model with either reaction or ash diffusion control, the time for complete conversion of grains (or when the ash layer first forms on the outside of the pellet) being τ_g .
- The rate of attack of the virgin core and of the grains is first order with respect to gaseous reactant.

Fig. 4 then illustrates the different stages through which a pellet passes according to this model. Note that when $\tau_c > \tau_g$ the grains at the surface of the pellet are completely converted before the attacking front reaches the center of the pellet, and consequently for part of the time three distinct composition zones are present in the pellet: an inner virgin core, an outer completely reacted shell, and in between partly reacted solid.

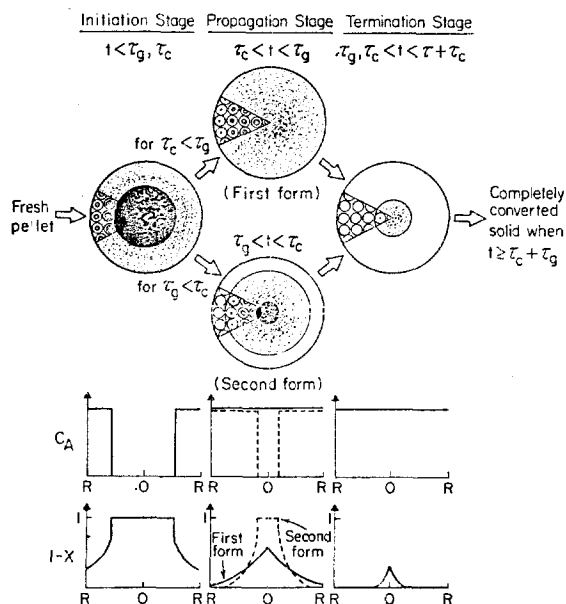


Fig. 4. Progressive stages in conversion of a pellet for the crackling core model.

Reflection also shows that the time for complete conversion of the pellet will be time needed for the attacking front to reach the center of the pellet plus the time for that grain to be converted, or

$$\tau = \tau_g + \tau_c \quad (10)$$

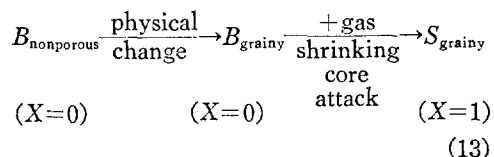
where, in the absence of diffusional resistance, τ_c is expressed by Eq. (1). Thus,

$$\tau_c \propto \frac{R}{k_c C_A} \quad (11)$$

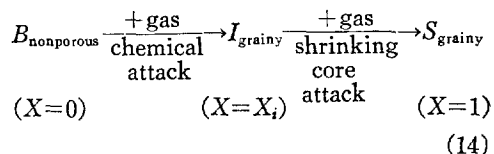
The time scales τ_c and τ are two independent parameters of this model, or equivalently Park and Levenspiel use the ratio of these times ω defined as

$$\omega = \frac{\tau_c}{\tau} = \frac{\tau_c}{\tau_c + \tau_g} \quad (12)$$

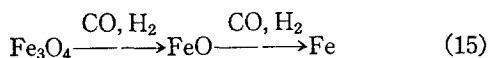
In some cases the attack of the virgin core, which is referred to as "crackling," only involves a physical change; in other cases it involves reaction to intermediate I of conversion X_i . Thus there are two possibilities, first the one reaction version of the crackling core model



and then the two reaction version



in which the intermediate conversion X_i is determined from the known stoichiometry of the two step reaction. For example, in the gaseous reduction of Fe_3O_4 , FeO appears as an intermediate product. For this two step reaction the stoichiometry indicates that a fourth of the oxygen is deleted in the crackling stage, or $X_i = 0.25$:



($X=0$) ($X=X_i=0.25$) ($X=1$)

Exact analytical expressions have been obtained for the conversion-time expressions for various pellet-grain geometries (Park¹⁵). Table 1 displays these for spherical pellet-spherical grain. Since the expressions are algebraic much like those for the shrinking core model, and since these are explicit with regard to conversion X , predictions with this model for macroscopic events such as performances of reactor, optimum design, etc. will be simple as well.

Comparison of the models

Some essential features of the two-parameter models are summarized and compared with those of the shrinking core model in Table 2. Let us consider this.

Graphical Representation.

Fig. 5 illustrates typical conversion-time curves and the regions where the curves belong (shaded area) for these models. For the grainy porous

pellet model (Fig. 5a) the approximate conversion-time expressions (Eqs. (8) and (9)) predict that these curves lie between the two extremes of the shrinking core model (Eqs. (2) and (3)), are always convex-up, and thus are not much different from the predictions of the shrinking core model. The crackling core model (Fig. 5b) predicts a much broader class of conversion-time behavior: convex-up curves, sigmoidal curves with an induction-like period, curves with a sudden initial jump, etc.

Sometimes the conversion-time curve may be used as a guide in choosing the proper model. This will be discussed in detail later.

Extreme Behavior for $\omega \cong 0$.

This extreme is approached either when the conversion of grains is extremely slow or when the diffusion (the grainy porous pellet model) or the crackling (the crackling core model) is very rapid. Here both of these models predict uniform conversion of grains throughout the pellet. Hence the time for complete conversion

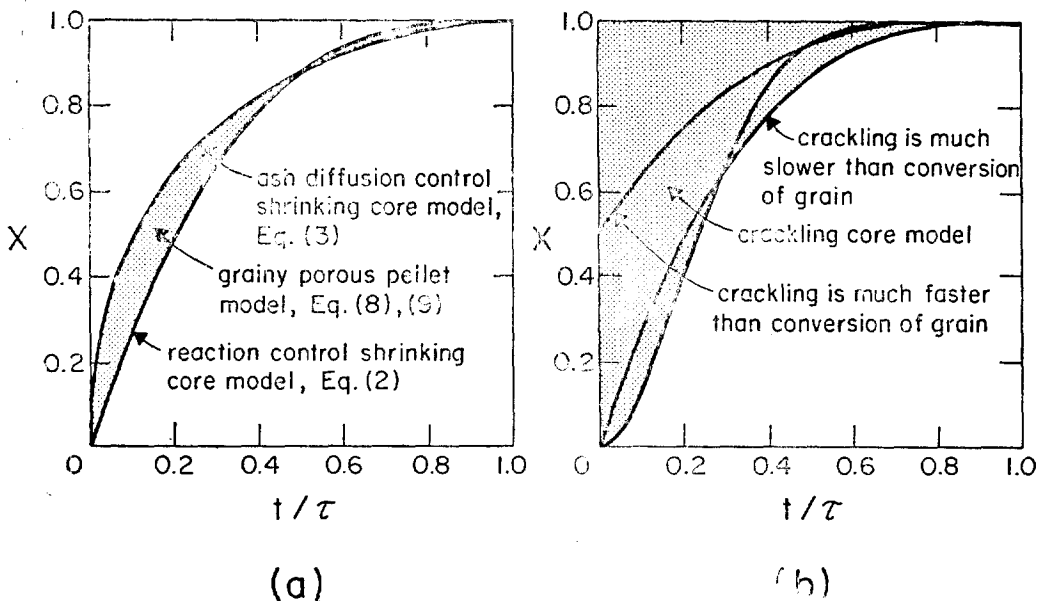


Fig. 5. Typical conversion-time curves for the two-parameter models.

(a) The grainy porous pellet model. (b) The crackling core model.

of pellet τ becomes that for the complete conversion of grains τ_g , and the conversion-time expressions are determined by the mechanism that controls the conversion of grains. For the conversion-time expressions for this extreme see Sohn and Szekely^{7,8)} and Park and Levenspiel¹⁰⁾.

For the two reaction version of the crackling core model the normalized time scale of Fig. 5b shows a sharp jump followed by a slow rise to 100% conversion. However, τ can be so long that all we observe is the sharp initial jump, which on the real time scale transforms into a steadily rising curve to X_{Ai} . Thus the crackling core model can fit systems where the conversion rises steadily to some limiting value which may be considerably below complete conversion.

Extreme Behavior for $\omega \cong 1$.

This extreme is approached when the conversion of grains is very fast relative to either the rate of gas diffusion into the pellet (the grainy porous pellet model) or the rate of crackling on the surface of virgin core (the crackling core model). The reacting grains are then confined to a very thin layer and the conversion of the pellet is mainly controlled by diffusion through the ash layer of the pellet (the grainy porous pellet model) or by the crackling (the

crackling core model). Thus in this extreme the grainy porous pellet model approaches the ash diffusion control shrinking core model (Eq. (3)) and the crackling core model approaches the reaction control shrinking core model (Eq. (2)).

Application to Stepwise Reactions.

The grainy porous pellet model provides no mechanistic view for stepwise reactions while the crackling core model does. It can be shown that many industrially important multistep reactions of solid particles may, for all practical purposes, be reduced to the two reaction version of the crackling core model.

Effect of Pellet Size.

In both models the time for complete conversion of grains τ_g is assumed to be independent of pellet size. Thus from Eqs. (4), (5) and (6), and from Eqs. (10) and (11) we obtain the following relationships for the effect of pellet size: For the grainy porous pellet model:

$$\tau \cong \tau_g + \tau_g \sigma^2 = a + bR^2 \quad (16)$$

For the crackling core model:

$$\tau = \tau_g + \tau_c = a + bR \quad (17)$$

Fig. 6 illustrates and compares these different predictions with those of the shrinking core model and the homogeneous reaction model.

Use of the models

When one has a gas-solid reaction system and when then the simple predictions of either the shrinking core model or the homogeneous reaction model fail to fit the system, one should try these two-parameter models. We will show in the following which of these models to choose to best fit the system and then how to fit the data with these models.

Selection of a Model.

This should be determined mainly by experimental observations. Thus if the solid is initially

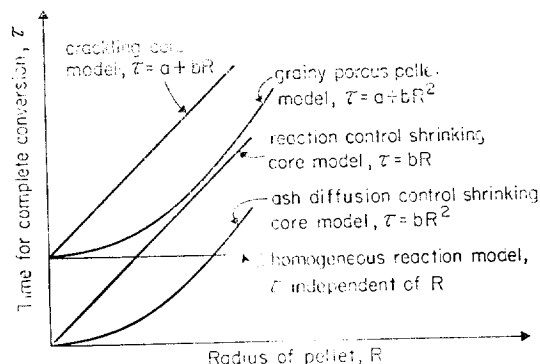


Fig. 6. Effect of pellet size on time for complete reaction for various models.

rather porous and the structural change due to reaction is rather mild, the grainy porous pellet model should be tried; on the other hand, if the solid is rather dense and a vigorous structural change occurs upon reaction, then one should try the crackling core model.

Unfortunately, there is not likely to be a clear cut criterion concerning the denseness of the reactant solid or the vigorousness of the structural change. Indeed sharp crackling fronts have been observed even in porous pellets which, initially consisting of large grains of dense reactant solid, then crackle away to leave fine grains behind, see the micrographs by Kor¹⁶⁾ for example.

A rather sensitive way to quantitatively differentiate between these two models may be first to best fit the data for each model as described in the following and then to see which of the predictions on the effect of pellet size (Eqs. (16) and (17)) better fits the experiment.

Also whenever an S-shaped conversion-time curve is obtained the crackling core model should be tried. It is the only model to date which can account for such induction-like behavior.

Fitting Data with the Models.

To fit these models to data one must choose

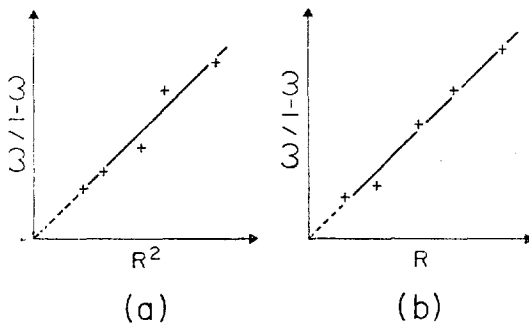


Fig. 7. Verification that the size dependency is as predicted by Eq. (15) or (16)
(a) The grainy porous pellet model.
(b) The crackling core model.

τ_g and ω for best fit using conversion versus time data for different sizes of pellets. This would be a simple matter requiring a one dimensional search for ω if τ_g is accurately known experimental data with very fine particles for which ω approaches zero¹¹⁾ Otherwise trial and error fitting must be used¹⁰⁾. Thus, 1) first assume τ_g , 2) find ω for each pellet size, and then 3) check whether the size dependency agrees with the prediction of the model.

However, since the time for complete conversion is usually uncertain and since the predictions of all models could well break down in this regime due to sintering, occlusion, etc., it is suggested that one use the following equivalent expressions for the size dependency: For the grainy porous pellet model

$$\frac{\omega}{1-\omega} = \frac{\tau_d}{\tau_g} \propto R^2 \quad (18)$$

For the crackling core model

$$\frac{\omega}{1-\omega} = \frac{\tau_c}{\tau_g} \propto R \quad (19)$$

Fig. 7 illustrates how, after fitting the data to find τ and ω , one should check whether Eq. (18) or (19) is satisfied.

Extensions to three parameter models

Through the preceding comparisons and discussion it has been shown that in their respective phenomenological view and extreme behavior these models represent two distinctly different extensions of the simple shrinking core model: thus, the grainy porous pellet model is an extension to the ash diffusion control shrinking core model and the crackling core model is an extension to the reaction control shrinking core model.

These models also have their respective extensions to three parameter models. These are the *varying-diffusivity porous pellet model* of Ishida

and Wen⁵⁾ (its metallurgical engineering version has been developed by Tien and Turkdogan⁶⁾) as an extension to the grainy porous pellet model and the *diffusion-influenced crackling core model* as a possible extension to the crackling core model.

Ishida and Wen⁵⁾ view that the effective diffusivity through the ash layer is different to that through the partly converted solid. On the other hand, the diffusion-influenced crackling core model views that the sharp crackling front still exists but the passage of gas through the crackled layer is retarded by diffusional resistance.

These multiple parameter models based on more detailed mechanistic views, however, introduce an additional parameter which is usually to be found by data-fitting, and thus are hardly useful for practical purposes. In fact, conversion versus time data obtained from a limited set of experiments are usually not sensitive enough to justify these multiple parameter models and indeed it has been repeatedly mentioned that simple models can equally well fit the data as more complex ones.

Conclusions

Two-parameter models and their predictions are compared for the reaction of solid particles. The grainy porous pellet model of Sohn and Szekely should be good for porous pellets with little structural change upon reaction. It predicts practically the same conversion-time behavior as the simple shrinking core model (see *Fig. 5a*), it predicts a size dependency given by $\tau = a + bR^2$, and it can account for a broad reaction front in the pellet, all the way from homogeneous conversion to ash diffusion control shrinking core.

The crackling core model of Park and Levenspiel should be useful for the reaction of dense solid particles which undergo a vigorous structural change upon reaction. It can account for both S-shaped and the ordinary convex-up conversion versus time curves (see *Fig. 5b*), it predicts a size dependency given by $\tau = a + bR$, it can account for multistep reactions of solids, it can fit data where the conversion rises steadily up to some intermediate conversion, often far below complete conversion of solid, and it can account for a broad reaction front, all the way from homogeneous conversion to reaction control shrinking core.

Table 1. Conversion expressions for the crackling core model
(Spherical pellet-spherical grain)

Reaction Control in Grain

$$\begin{aligned} \text{Initiation stage: } & 1-X = 1 - \frac{1}{\omega} \left(1 - \frac{t}{\tau}\right)^3 + \frac{(1-X_i)}{\omega^3(1-\omega)^3} \left[\frac{3}{4} \left(1 - \frac{t}{\tau}\right)^2 [(1-\omega)^4 - (1-\omega - \frac{t}{\tau})^4] \right. \\ & \left. - \frac{6}{5} \left(1 - \frac{t}{\tau}\right) [(1-\omega)^5 - (1-\omega - \frac{t}{\tau})^5] + \frac{1}{2} [(1-\omega)^6 - (1-\omega - \frac{t}{\tau})^6] \right] \\ (t \leq \tau_g, \tau_c) & \end{aligned}$$

$$\begin{aligned} \text{Propagation stage:} & \\ \text{First form: } & 1-X = \frac{(1-X_i)}{\omega^3(1-\omega)^3} \left[\frac{3}{4} \left(1 - \frac{t}{\tau}\right)^2 [(1-\frac{t}{\tau})^4 - (1-\omega - \frac{t}{\tau})^4] - \frac{6}{5} \left(1 - \frac{t}{\tau}\right) [(1-\frac{t}{\tau})^5 \right. \\ & \left. - (1-\omega - \frac{t}{\tau})^5] + \frac{1}{2} [(1-\frac{t}{\tau})^6 - (1-\omega - \frac{t}{\tau})^6] \right] \\ (\tau_c < t \leq \tau_g) & \end{aligned}$$

$$\text{Second form: } 1-X = \left(1 - \frac{1}{\omega} \frac{t}{\tau}\right)^3 + \frac{(1-X_i)(1-\omega)}{\omega^3} \left[\frac{3}{4} \left(1 - \frac{t}{\tau}\right)^5 - \frac{6}{5} (1-\omega) \left(1 - \frac{t}{\tau}\right) \right]$$

$$(\tau_g < t \leq \tau_c) \quad + \frac{1}{2}(1-\omega)^2]$$

$$\text{Termination stage: } 1-X = \frac{(1-X_i)(1-\frac{t}{\tau})^6}{20\omega^3(1-\omega)^3}$$

($\tau_g, \tau_c < t \leq \tau_g + \tau_c$)

Ash Diffusion Control in Grain

$$\text{Initiation stage: } 1-X = (1-\frac{1}{\omega}\frac{t}{\tau})^3 + \frac{(1-X_i)(1-\omega)}{\omega^3} [Z(y)]_i^{y_i}$$

($t \leq \tau_g, \tau_c$)

Propagation stage:

$$\text{First form: } 1-X = \frac{(1-X_i)(1-\omega)}{\omega^3} [Z(y)]_s^{y_s}$$

($\tau_c < t \leq \tau_g$)

$$\text{Second form: } 1-X = (1-\frac{1}{\omega}\frac{t}{\tau})^3 + \frac{(1-X_i)(1-\omega)}{\omega^3} [\frac{3}{5}(1-\frac{t}{\tau})^2 - \frac{13}{14}(1-\omega)(1-\frac{t}{\tau}) + \frac{21}{55}(1-\omega)^2]$$

($\tau_g < t \leq \tau_c$)

$$\text{Termination stage: } 1-X = \frac{(1-X_i)(1-\omega)}{\omega^3} [Z(y)]_y^0$$

($\tau_g, \tau_c < t \leq \tau_g + \tau_c$)

where

$$Z(y) = (1-\frac{t}{\tau})^2(3y^6 - \frac{18}{5}y^5) + (1-\omega)(1-\frac{t}{\tau})(8y^9 - \frac{45}{2}y^3 - \frac{108}{7}y^7) + (1-\omega)^2(6y^{12} - \frac{288}{11}y^{11} + \frac{189}{5}y^{10} - 18y^9)$$

$y =$ dummy variable

$$y_s = \frac{1}{2} + \cos \frac{\theta_s + 4\pi}{3}; \theta_s = \cos^{-1}[\frac{2}{1-\omega}(\frac{t}{\tau}) - 1], \quad 0 \leq \theta_s \leq \pi$$

$$y_c = \frac{1}{2} + \cos \frac{\theta_0 + 4\pi}{3}; \theta_0 = \cos^{-1}[\frac{2}{1-\omega}(\frac{t}{\tau} - \omega) - 1], \quad 0 \leq \theta_0 \leq \pi$$

REFERENCES

1. S. Yagi and D. Kunii, *5th Symposium (International) on Combustion*, Reinold, New York 1955, pp. 231; *Chem. Eng. (Japan)*, **19** (1955), 500.
2. W.M. McKewan, *Trans. Met. Soc. AIME*, **212** (1958), 791-793.
3. O. Levenspiel, "Chemical Reaction Engineering," 2nd ed., Wiley, New York, 1972, Chap. 12.
4. R.H. Spitzer, F.S. Manning and W.O. Philbrook, *Trans. Met. Soc. AIME*, **236** (1966), 726-742.
5. M. Ishida and C.Y. Wen, *AICHE J.*, **14** (1968), 311-317.
6. R.H. Tien and E.T. Turkdogan: *Met. Trans.*, **3** (1972), 2039-2048.
7. H.Y. Sohn and J. Szekeley: *Chem. Engng. Sci.*, **27** (1972), 763-778.
8. H.Y. Sohn and J. Szekeley: *Chem. Engng. Sci.*, **29** (1974), 630-634.
9. R.L. Pigford and G. Sliger, *Ind. Eng. Chem. Proc. Des. Dev.*, **12** (1973), 85-91
10. J.Y. Park and O. Levenspiel *Chem. Engng. Sci.*, **30** (1975), 1207-1214.
11. J. Szekeley, C.I. Lin and H.Y. Sohn, *Chem. Engng. Sci.*, **28** (1973), 1975-1989.
12. J. Szekeley and N.J. Themelis, *Rate Phenomena in Applied Metallurgy*, Wiley, New York, 1971, pp. 630.

著 者 略 歷

朴 晋用 博士는 1967年 서울工大 化學工學科를 卒業하고 軍 服務後 嶺南化學 蔚山工場에 勤務中 1971년에 渡美하여 1972年 University of Idaho 에서 液體의 混合에 關한 論文으로 碩士學位를 받았다. 그後 Oregon State University 로

옮겨 1976年 氣固系 反應 및 觸媒의 非活性化에 關한 論文으로 博士學位를 받고 University of Florida 에 招聘教授로 在職中 歸國하여 現在 서울工大 化學工學科에 助教授로 在職하고 있다.

朴 博士는 反應工學, 流動化工學 및 混合現象에 關한 研究經歷을 갖고 있으며 앞으로 環境問題에도 積極 參與할 計劃이다.

